High-frequency EPR spectra of a molecular nanomagnet: Understanding quantum tunneling of the magnetization

Anne Laure Barra
Laboratoire des Champs Magnetiques Intenses, CNRS, Boite Postale 166, Grenoble Cedex 9, France

Dante Gatteschi and Roberta Sessoli
Department of Chemistry, University of Florence, Via Maragliano 75, 0144 Firenze, Italy

(Received 31 January 1997)

EPR spectra have been recorded in very high fields up to 25 T, and at high frequency up to 525 GHz, on a polycrystalline sample of $[Mn_{12}O_{12}(CH_3COO)_{16}(H_2O)_4]\cdot 2CH_3COOH\cdot 4H_2O$ (Mn12ac), a molecular cluster behaving like a nanomagnet. The simulation of the spectra has provided an accurate determination of the parameters of the spin Hamiltonian $H=\mu_B\mathbf{H}\cdot\mathbf{g}\cdot\mathbf{S}+D[S_z^2-1/3S(S+1)]+B_4^0O_4^0+B_4^4O_4^4$, where $O_4^0=35S_z^4-30S(S+1)S_z^2+25S_z^2-6S(S+1)+3S^2(S+1)^2$ and $O_4^4=1/2(S_+^4+S_-^4)$: $D=-0.46(2)\text{cm}^{-1}$, $B_4^0=-2.2(2)\times10^{-5}$ cm^{-1}, and $B_4^4=\pm4(1)\times10^{-5}$ cm^{-1}. The presence of the fourth-order term in the total spin justifies the irregularities in the spacing of the jumps, recently observed in the hysteresis loop of Mn12ac and attributed to acceleration of the relaxation of the magnetization due to quantum tunneling between degenerate M states of the ground $S=10$ multiplet of the cluster. The term in $(S_+^4+S_-^4)$ is responsible for the transverse magnetic anisotropy and plays a crucial role in the mechanism of quantum tunneling. The high-frequency-EPR spectra have shown its presence and quantified it. [S0163-1829(97)08237-4]

I. INTRODUCTION

Quantum tunneling of the magnetization (QTM) is one of the candidates to test the possibility of observing quantum effects in macroscopic (or perhaps more appropriately mesoscopic) objects.[1,2] The interest for this kind of problem is certainly a theoretical one, aimed at understanding the limits of validity of quantum mechanics, but in principle also a practical one. In fact small magnetic particles are used to store information and it would be desirable to have a knowledge of the lower limit of the size which can be achieved. The requisite for storing information is that the magnetization is either up or down, but if tunneling occurs, the stored information is lost. Therefore the limit size for observing QTM should be known.[3]

Many attempts were made to produce even smaller magnets,[4,5] but most efforts were plagued by the impossibility of obtaining ensembles of identical nanoparticles which could be kept well separated from each other in order to minimize interactions which would hamper the observation of QTM. Techniques of molecular chemistry on the other hand suggested a different approach, using large molecular clusters as single nanomagnets.[6] Surprisingly enough it was found that nanomagnetic properties can be observed in relatively small clusters, comprising only eight metal ions.[7]

The main advantage that molecular clusters have compared to other systems, like small magnetic particles either of metals or of oxides, or even ferritin, is that they are absolutely monodisperse, their structure is perfectly known from x-ray techniques, they can be well separated one from the other by dissolving them in appropriate solvents and polymer films.[8,9]

The most accurately investigated system so far is $[Mn_{12}O_{12}(CH_3COO)_{16}(H_2O)_4]\cdot 2CH_3COOH\cdot 4H_2O$, Mn12ac, which has the structure shown in Fig. 1. It comprises an external ring of eight manganese(III) ions ($S=2$) and an internal tetrahedron of four manganese(IV) ions ($S=3/2$). The cluster has a crystal imposed S_4 symmetry.[10] It has a ground $S=10$ state, which can be loosely described setting all the manganese(III) spins up ($S=8\times2=16$) and all the manganese(IV) spins down ($S=-4\times3/2=-6$). The ground multiplet is split by the tetragonal symmetry to leave the $M=\pm10$ components lying lowest.[11] At low temperature these are the only populated levels.

Mn12ac is a molecular cluster for which slow relaxation of the magnetization was detected at low temperature,[11] similar to the blocking temperature of superparamagnets. In fact, the relaxation time was found to follow a thermally activated behavior down to 2 K, according to the equation $\tau=\tau_0\exp(A/kT)$, with a pre-exponential factor $\tau_0=2.1\times10^{-7}$ s, and an energy barrier $A/k=61$ K.[12] In this range of temperature the cluster behaves like a single-molecule

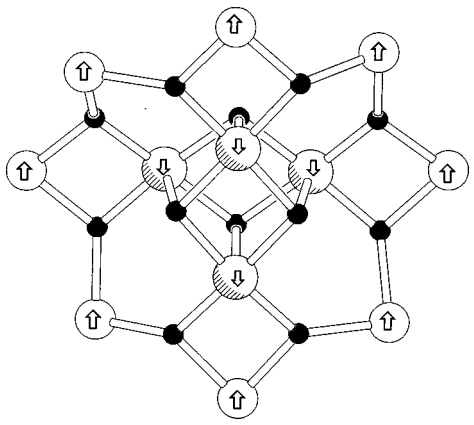

FIG. 1. Sketch of the structure of the magnetic core of the cluster. The arrows show the spin structure of the ground $S=10$ state.

magnet, showing also hysteresis effects. This gives the exciting perspective of storing information at the molecular level.

Below 2 K, the relaxation time becomes independent of temperature, suggesting a quantum tunneling mechanism.[13] In zero applied magnetic field the M levels are degenerate in pairs and resonant QTM may occur between $M=-10$ and $M=+10$, $M=-9$ and $M=+9$, etc. This mechanism seems to be active also at higher temperature as suggested by the dramatic increase of the relaxation time observed by applying a weak magnetic field.[14] The increase of the relaxation time with an applied field is certainly surprising, because usually the reverse is observed in superparamagnets. In fact in a thermally activated process the application of the external field decreases the height of the barrier, and makes the relaxation of the magnetization faster. On the other hand, if thermally activated relaxation coexists with QTM this unexpected behavior may find a justification. In fact, when the applied field removes the degeneracy quantum tunneling is suppressed with a dramatic increase in the relaxation time. A confirmation to this came from the fact that the relaxation time was found to decrease dramatically for values of the external field which put the M and the $-M+n$ levels at the same energy.[15,16] In this case pairs of degenerate levels are again present, and QTM is efficient, thus justifying the increase in the relaxation rate. Therefore a model which implies tunneling effects not only involving the lowest lying $M=\pm 10$, but also the excited $M=\pm 9, \pm 8$, etc. has been postulated, in a thermally assisted QTM.[17]

In order to develop a quantitative understanding of the mechanism of QTM in Mn12ac several points still need to be clarified. The first is the height of the barrier for the reorientation of the magnetization. The experimentally determined value from ac susceptibility measurements should be compared with that obtained through more direct techniques, like EPR. In fact we previously reported high-frequency EPR (HF-EPR) spectra monitoring the $M=-10 \rightarrow M=-9$ transition and from that we obtained a zero-field splitting parameter $D=-0.5\ \mathrm{cm}^{-1}$.[11] When the system is in the ground $M=-10$ level in order to invert the magnetization it must go to the degenerate $M=+10$ level. In the thermally activated process this can be done by climbing up the ladder of levels to $M=0$, and then descending.[18] Therefore the height of the barrier is equivalent to the energy separation between the $M=-10$ and $M=0$ levels in zero field, which is given by $A=S^2|D|$. With the D parameter of the EPR spectra we calculated an energy barrier for the reorientation of the magnetization $A/k=72$ K, which is not far from that obtained by the measurement of the relaxation time, $A/k=61$ K. However if the difference is significant this may be an indication of possible short cuts for relaxation determined by QTM between excited levels. Therefore a more accurate set of EPR data is needed.

The second point to be clarified is that in order to theoretically justify QTM it is necessary to identify nonzero matrix elements of the zero-field Hamiltonian connecting the $\pm M$ levels. In an equivalent way it is necessary to identify a transverse (in-plane) magnetic anisotropy in order to justify QTM. In the tetragonal symmetry of the cluster, this cannot be provided by the quadratic crystal-field operator, which is diagonal. However, higher-order crystal-field effects may be included, the smallest being the fourth-order terms which mix states differing by four in M. They determine an in-plane magnetic anisotropy and therefore can provide a coupling between the $M=+10$ and $M=-10$ levels in high-order perturbation. The same terms can couple the excited M states more efficiently. For instance they may couple in first order the $M=\pm 2$ levels. Several attempts[17,19] are currently being made to theoretically justify the observed relaxation times of the cluster, with and without an applied magnetic field, by introducing fourth-order crystal-field parameters, whose presence up to now has not been proved. EPR in principle, can directly provide the values of the parameters which can be compared with those required by theory.

The previously reported HF-EPR spectra[11] were measured on polycrystalline powders partially oriented by the strong magnetic field required by the high-frequency spectrometer. We have now performed more accurate experiments at frequencies ranging from 150 to 525 GHz in field up to 25 T on a blocked polycrystalline powder sample at various temperatures in order to determine the presence of fourth-order components of the crystal field. The results that we wish to report here, have allowed a quantification of the fourth-order terms in the spin Hamiltonian and show how powerful a tool HF-EPR is for obtaining information on transition-metal ions and on systems with an even number of unpaired electrons.

II. EXPERIMENTAL PROCEDURE

A. Physical measurements

As no single crystals large enough are available, all the HF-EPR measurements have been performed on polycrystalline powders, synthesized as previously reported.[10,20] The powder was pressed into a pellet to prevent orientation of the microcrystallites in the magnetic field. A small sample of diphenyl-dipicryl-hydrazide (dpph) was added to calibrate the magnetic field.

A first series of measurements was performed on the standard HF-EPR Grenoble spectrometer.[21] In this setup the exciting frequency is provided by a far-infrared laser, optically pumped by a CO_2 laser (Edinburgh Instruments), which is sent with oversized light pipes to the sample. A small modulation field is superimposed to the main one, with an oscillating frequency of 10 kHz. The transmitted light is detected by a hot electron InSb bolometer (QMC Instruments). The main magnetic field is provided by a superconducting magnet (Cryogenics Consultant), working up to 12 T at 4.2 K. A variable temperature insert (Oxford Instruments) enables one to work from 1.6 to 300 K.

A second series of measurements was performed moving the whole setup in order to replace the superconducting magnet by the hybrid magnet of the LCMI, in order to reach a maximum field of 30 T. Due to the important stray magnetic field of this magnet, the laser source as well as the detection system needed to be much farther (several meters) from the sample than in the standard setup, resulting in a reduced signal-to-noise ratio. In that case, the spectra were recorded keeping the superconducting magnet at a constant field and sweeping only the resistive magnet.

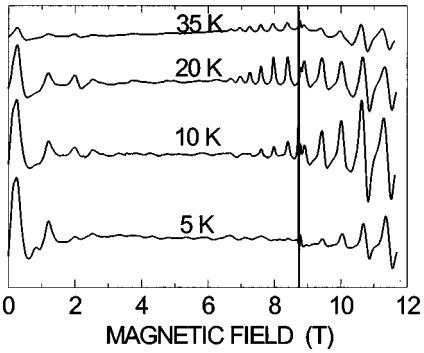

FIG. 2. Polycrystalline powder HF-EPR spectra of Mn12ac at 245 GHz at different temperatures. The narrow signal is given by DPPH ($g=2.0037$).

B. Calculations

The powder EPR spectra have been simulated using a program developed by Jacobsen *et al.*,[22] which calculates the matrix associated to the effective Hamiltonian for each value of the magnetic field and each orientation of the sample. This kind of treatment was necessary as the zero-field splitting term was too large to be considered as a perturbation of the Zeeman interaction. The Hamiltonian matrix must be computed for the basis of 21 functions corresponding to the S multiplet, for a given value and orientation of the field and diagonalized. A powder average is then performed.

III. RESULTS AND DISCUSSION

A. EPR Spectra

Polycrystalline powder spectra of Mn12ac were recorded with exciting frequencies of 158, 245, 349, 428, and 525 GHz, with a spectrometer equipped with a 12 T magnet. The spectra recorded at 245 GHz are shown in Fig. 2. The spectra at 35 K show many feature at low field corresponding to the fine structure expected for an $S=10$ multiplet split in zero field by crystal-field effects. On decreasing temperature the relative intensities of the transitions change dramatically, with an increase of the lowest field parallel component at 0.25 T, and an increase of the high-field perpendicular transition at 11.47 T. This is the result of the depopulation of the higher M levels, due to the large Zeeman energy. In fact for 245 GHz the Zeeman energy corresponds to $\sim$12 K, and at 4.2 K essentially only the lowest $M=\pm 10$ states are populated. Therefore the transition corresponding to $M=-10\rightarrow M=-9$ gains in intensity on decreasing temperature. This occurs at low field for H parallel to the tetragonal axis, and at high field for H perpendicular. This confirms that the zero-field splitting in Mn12ac is negative and that therefore the magnetic anisotropy is of the Ising type. The resonance field of the lowest field transition corresponds well to that previously reported for the oriented samples.

The spectra recorded at higher frequencies are simpler to be assigned on a qualitative basis, because they move towards the high-field approximation. On increasing frequencies the high-field transitions are however progressively lost, due to the fact that they move outside the available magnetic field range. In fact for an exciting frequency of 525 GHz the resonance field of the free electron is 18.73 T. For a zero-field splitting $|D|\cong 0.5$ cm^{-1} the highest field parallel transition can be at 28.9 T. Therefore it was necessary to use a hybrid magnet capable of reaching 30 T. The spectra recorded with the hybrid magnet at 349 GHz are shown in Fig. 3(a). The low-field region of the spectra is similar to that observed with the standard superconducting magnet, but the high-field region now shows a rich structure. Some doubling of the peaks seems to be due to aging of the samples. Some experiments have been repeated on a fresh sample and the spectrum is substantially the same, except for the extra peaks. Larger polarization effects are observed on decreasing temperature since in this case the Zeeman energy is 16 K. At 4.2 K the lowest parallel transition is observed at 1.74 T, and the highest perpendicular transition at 18.0 T.

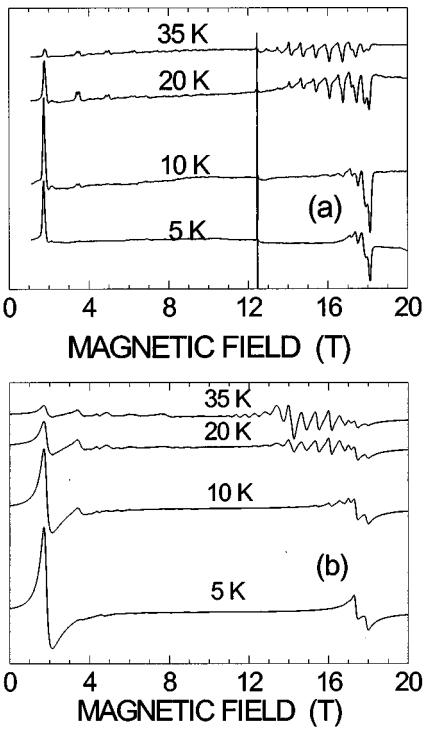

FIG. 3. Polycrystalline powder HF-EPR spectra of Mn12ac at 349 GHz at different temperatures: (a) experimental, (b) calculated with the parameters mentioned in the text.

The separations between neighboring parallel lines at relatively high temperature are not constant throughout the spectrum. For instance at 349 GHz the lowest field parallel transitions are observed at 1.81, 3.47, 4.92, 6.23, and 7.37 T, with the corresponding separations 1.66, 1.45, 1.31, and 1.14 T.

The spectra recorded at 525 GHz are shown in Fig. 4(a). The lowest parallel transition is observed at 8.03 T, and the highest perpendicular at 24.2 T. The polarization effects here are remarkable even at high temperature, because the Zeeman energy is $\sim$26 K.

B. Simulation strategy

The fit of the spectra of an $S=10$ multiplet even in tetragonal symmetry is by no means a simple task. The spin Hamiltonian[23] can be expressed as

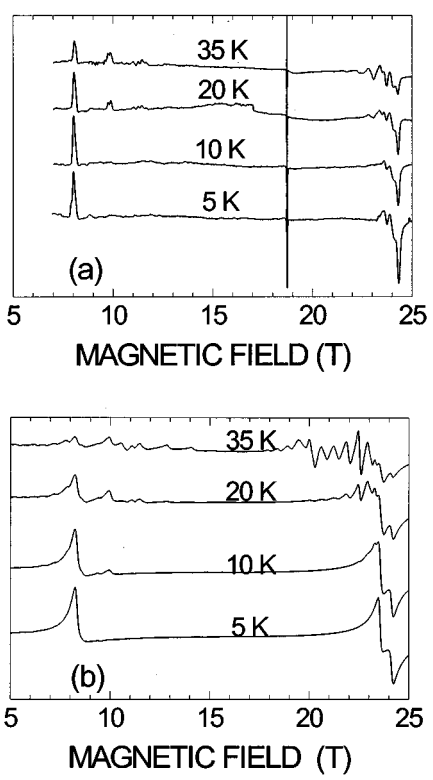

FIG. 4. Polycrystalline powder HF-EPR spectra of Mn12ac at 525 GHz and different temperatures: (a) experimental, (b) calculated with the parameters mentioned in the text.

$$H=\mu_B\mathbf{H}\cdot\mathbf{g}\cdot\mathbf{S}+D[S_z^2-1/3S(S+1)]+B_4^0O_4^0+B_4^4O_4^4, \tag{1}$$

where $O_4^0=35S_z^4-30S(S+1)S_z^2+25S_z^2-6S(S+1)+3S^2(S+1)^2$ and $O_4^4=1/2(S_+^4+S_-^4)$. In principle it would be possible to include also higher-order crystal-field terms, with O_n operators with $n=6,8,\ldots,20$. However we restricted ourselves to fourth-order terms for the sake of simplicity.

The fit of the spectra requires the adjustment of fine parameters, namely $g_\parallel$, $g_\perp$, D, B_4^0, B_4^4. Since a cycle with a given set of parameters requires ~40 min on our workstation, it is necessary to try to have some preliminary guess of the values of the parameters, and of their relevance to the computed spectra. D is known to be ~ -0.5 cm^{-1}, therefore its variation was limited to a narrow range around this value. The effect of the term in D is that of splitting the $S=10$ multiplet in pairs of $\pm M$ levels. In the high-field approximation, i.e, when the Zeeman energy is much larger than $(2S+1)|D|$, the spectrum should consist of 20 parallel and 20 perpendicular $M\rightarrow M+1$ transitions, with resonance fields

$$H_r(M)=\frac{g_e}{g}[H_0-(2M+1)D'], \tag{2}$$

where $D'=D/(g_e\mu_b)$for parallel and $D'=D/(2g_e\mu_b)$ for perpendicular transitions an M ranges from $-S$ to $S-1$. The neighboring lines are therefore regularly spaced by $2D/(g_e\mu_B)$ for the field parallel and by $D/(g_e\mu_b)$ for the field perpendicular to the tetragonal axis. The observed transitions were seen not to follow these conditions even at the highest available frequency, suggesting that the inclusion of only the quadratic term is not sufficient to satisfactorily reproduce the spectra. In fact attempts to fit the spectra without introducing quartic terms were completely unsuccessful.

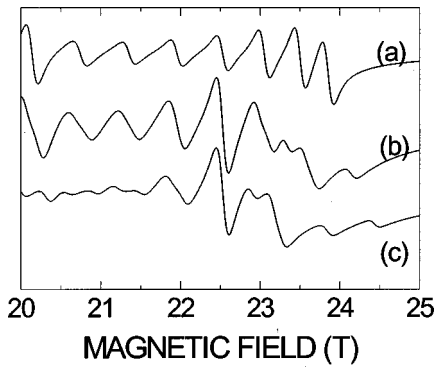

FIG. 5. High-field region of the spectrum at 525 GHz and 30 K calculated with $D=-0.46$ cm^{-1}, $B_4^0=-2.2\times10^{-5}$ cm^{-1}, and $B_4^4=0$ (a), 4×10^{-5} (b), and 8×10^{-5} cm^{-1} (c).

The introduction of nonzero B_4^0 changes the diagonal energies of the M levels, mostly affecting the parallel transitions. The ones which are most affected are those with large $|M|$, therefore nonzero B_4^0 will change the resonance fields and the separations of the low-field transitions, corresponding to $-10\rightarrow-9$, $-9\rightarrow-8$, etc. In the strong-field limit, and assuming that the quartic term is small compared to the quadratic term the resonance fields are given by

$$H_r(M)=\frac{g_e}{g}[H_0-(2M+1)(D'-3275B_4^{0'})-35(4M^3+6M^2+4M+1)B_4^{0'}], \tag{3}$$

where $B_4^{0'}=B_4^0/(g_e\mu_B)$. Provided that D is negative, as in the present case, a negative B_4^0 increases the separation between the lines on decreasing the field, while the opposite trend is observed for positive B_4^0.

A nonzero B_4^4 determines a mixing of M levels. Therefore it essentially affects the perpendicular spectra. In Fig. 5 we show the effect of introducing nonzero B_4^4 on the high-field perpendicular spectra corresponding to a frequency of 525 GHz.

C. Spectral fit

The D and B_4^0 terms of the spin Hamiltonian can be determined analytically by looking at the spacing of the parallel transitions in the spectra recorded at the highest frequencies, 349 and 525 GHz, but the B_4^4 term requires a full simulation of the spectra. A satisfactory agreement with experimental spectra, as shown in Figs. 3 and 4 for 349 and 525 GHz, respectively, has been achieved with the following parameters: $g_\parallel=1.93(1)$, $g_\perp=1.96(1)$, $D=-0.46(2)$ cm^{-1}, $B_4^0=-2.2(2)\times10^{-5}$ cm^{-1}, $B_4^4\pm4(1)\times10^{-5}$ cm^{-1}.

While the position of the lines is well reproduced in the simulated spectra the shape of the lines differs significantly. This can result for the experimental setup, which allows the presence of standing wave between different parts of the spectrometer, resulting in a mixing of a pure absorption

spectrum with a dispersion one. However, we do not expect this effect to be dramatic, and poor simulation of the line shape can be also due to the simulation program used, which does not allow us to introduce an anisotropic linewidth.

In the spin Hamiltonian (1) S_z^2 is present both in the quadratic and the quartic terms. If we rewrite the zero-field splitting terms as

$$H=\alpha S_z^2+\beta S_z^4+\gamma(S_+^4+S_-^4)+\text{const terms}, \tag{4}$$

where $\alpha=D-[30S(S+1)-25]B_4^0$, $\beta=35B_4^0$, $\gamma=1/2B_4^4$, we get $\alpha=-0.39(3)$ cm^{-1}, $\beta=-7.7(7)\times10^{-4}$ cm^{-1}, and $\gamma=\pm2.0(5)\times10^{-5}$ cm^{-1}. The second-order zero-field splitting parameter, which in this notation is α rather than D, is distinctly lower than estimated from other EPR measurements performed[11] on this system. This difference comes from the fact that the initial estimation was obtained from the position of the first low-field line considering only the effect of the second-order terms, and in the strong-field approximation.

The spin-Hamiltonian parameters for the cluster can be related to the parameters of the individual ions provided that the ground state is correctly known. The complexity of this spin system, which comprises 10^6 spin states, does not allow a quantitative estimation of the energies and an accurate description of the ground states. However it is possible to make an educated guess, using qualitative considerations. In scheme **SI** we assume that the ground $S=10$ is reasonably well described by the combination of $S_A=16$ for the eight manganese(III) and $S_B=6$ for the four manganese(IV). In this case the g values are given by[24]

$$g_{s=10}=1.5455g_{\mathrm{Mn(III)}}-0.5455g_{\mathrm{Mn(IV)}}. \tag{5}$$

$g_{\mathrm{Mn(IV)}}$ is expected to be rather isotropic, while larger anisotropy is expected for manganese(III). Therefore the observed anisotropy of the cluster must reflect the anisotropy of the manganese(III) ions, and the relative orientation of the individual **g** tensors. All the manganese(III) ions are elongated octahedral, with the elongation axes essentially parallel to the tetragonal axis. Therefore the **g** anisotropy of the cluster should be of the same sign as that of elongated manganese(III) ones, namely $g_\parallel<g_\perp$, as observed.[25] If we assume $g_{\mathrm{Mn(IV)}}=2$, isotropic, we calculate $g_{\parallel\mathrm{Mn(III)}}=1.95$, $g_{\perp\mathrm{Mn(III)}}=1.97$.

The ground $S=10$ state of the cluster has also been described choosing a different coupling scheme, assuming that the antiferromagnetic coupling between the four pairs of manganese(III) and manganese(IV) ions bridged by two oxo groups is dominant.[20] In this scheme, which we label as **SII**, there are four pairs in the ground $S=1/2$ which are coupled to give an intermediate $S_A=4\times1/2=2$, which are then ferromagnetically coupled to the remaining four manganese(III) ions to give a ground $S=10$ state. In this case the g tensor for $S=10$ is expected to be given by

$$g=1.2g_{\mathrm{Mn(III)}}-0.2g_{\mathrm{Mn(IV)}}. \tag{6}$$

The same qualitative conclusion as in **SI** applies in **SII**.

The projection of the zero-field splitting parameter D of the cluster on those of the single ions was previously suggested[24] and assuming that it is dominated by the contribution of the Jahn-Teller distorted manganese(III) ions, the following condition must hold in **SI**:

$$D=0.2276D_{\mathrm{Mn(III)}}. \tag{7}$$

From the experimental value of the zero-field splitting parameter and Eq. (6) we calculate $D_{\mathrm{Mn(III)}}=-2$ cm^{-1}. This can be compared to the value $D=-3.4$ cm^{-1} observed for manganese (III) in rutile[26] and $D=-4.6$ cm^{-1} observed in a monomeric complex, $\mathrm{Mn}(dbm)_3$.[27] If on the other hand, we use the g values of manganese(III) calculated above to estimate the zero-field splitting parameter with the relation $D=1/2\lambda[g_\parallel-g_\perp]$,[22] we obtain $D=-1.8$ cm^{-1}. If we apply **SII** then

$$D=0.1263D_{\mathrm{Mn(III)}} \tag{8}$$

yielding $D_{\mathrm{Mn(III)}}=-3.64$ cm^{-1}. Therefore the observed D parameter appears to be fully compatible with single manganese(III) ion anisotropy.

The analysis of the fourth-order terms was previously given for the O_4^4 terms both in **SI** and **SII**.[28] In this case, neglecting exchange determined contributions, the fourth-order terms must be given by the contributions of the $\mathrm{Mn^{III}}$ ions, b_4^n, because $\mathrm{Mn^{IV}}$ has $S=3/2$. It was found that

$$B_4^n=b_4^n/861, \tag{9}$$

$$B_4^n=b_4^n/1211, \tag{10}$$

for **SI** and **SII**, respectively. Using Eq. (9) and the parameters of the fit we obtain $b_4^4=0.03$ cm^{-1}. The comparison can again be made with the spectra reported for rutile, for which only the cubic parameter $a=0.16$ cm^{-1} was reported. Since the cubic parameter is given by[23] $a=24b_4^4$ the agreement can be considered as encouraging.

D. Hints to the mechanism of QTM

With the above parameters the height of the barrier, corresponding to the energy difference between the lowest $M=\pm10$ and the highest $M=0$ level, is calculated as $A/k=67.1$ K, which is in better agreement but still larger than the value obtained[12] from the fitting of the relaxation data, $A/k=61$ K. It is possible to justify a lower barrier obtained for the relaxation measurements if it is assumed that QTM is particularly efficient between the higher M levels. In this case they might provide an efficient shortcut for the relaxation of the magnetization also in the thermally activated regime. In fact QTM is favored when pairs of M states are degenerate. This is expected to occur at regular spacing symmetric around zero field, see Fig. 6, if the term in S_z^4 is not taken into account. Some authors have shown that regular spacing between the steps in the magnetization curve is observed if the field induction $B=H+4\pi M$ is considered as the local field experienced by the cluster.[15] We believe that the local field is more complicated than the average macroscopic internal field, B, and recent ac susceptibility data show that the regular spacing is not strictly observed.[29] Figure 6(b) shows the level crossings calculated with the second- and fourth-order terms obtained from the present investigation.

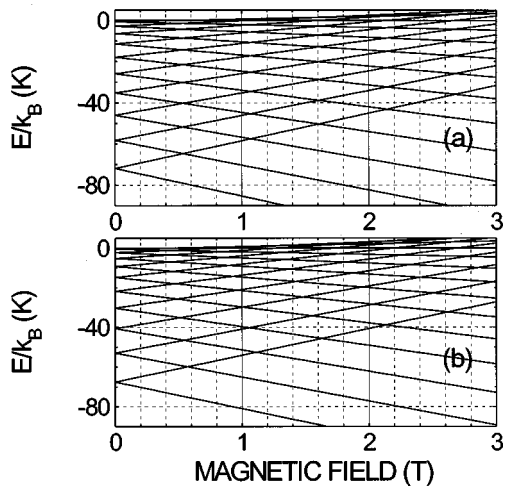

FIG. 6. Calculated splitting of the M levels of an $S=10$ multiplet with $D=-0.5$ cm^{-1} and $B_4^0=B_4^4=0$ (a), and with $D=-0.46$ cm^{-1}, $B_4^0=-2.2\times10^{-5}$ cm^{-1}, $B_4^4=4\times10^{-5}$ (b).

In this case the crossings of the different M levels occur at different field values. In particular the crossings involving levels with large M occur at higher fields than those involving levels with small M, and the spacing reduces on increasing the field. If the local field experienced by the cluster is precisely known, and the resonances sufficiently narrow, we could deduce from Fig. 6(b) which levels are mainly involved in the process of tunneling at the different temperatures.

The term in $(S_+^4+S_-^4)$ of the spin-Hamiltonian mixes state differing in M by multiples of four and can therefore induce tunneling. However some term linear in S_+ and S_- must be present in order to justify the presence of steps for any field crossings. Recently Fort *et al.*[30] have shown that the spin Hamiltonian deduced from HF-EPR spectra reproduces well the field dependence of the relaxation time. The selection rule $\Delta M=4n$ can be eased if a small transverse field, dipolar, external, or hyperfine, is present, but the order of magnitude of the tunneling rate is provided by the magnetocrystalline anisotropy evaluated by HF-EPR.

IV. CONCLUSIONS

The present results showed that HF-EPR is a unique tool for the determination of the crystal-field parameters in large spin clusters. In the particular compound of interest here the analysis of the spectra recorded in very high magnetic field allowed the determination of the parameter of the fourth-order spin operators S_z^4 and $(S_+^4+S_-^4)$. The first term could partially justify some irregularities observed in the steps of the magnetic quantum hysteresis of Mn12ac, while the second one provided evidence of the presence of an in-plane anisotropy, which can in principle justify the observation of QTM at low temperature.

[1] P. C. E. Stamp, E. M. Chudnovsky, and B. Barbara, Int. J. Mod. Phys. B **6**, 1355 (1992).

[2] *Quantum Tunneling of the Magnetization*, edited by L. Gunther and B. Barbara, NATO ASI Series E Vol. 301 (Kluwer, Dordrecht, 1995).

[3] D. D. Awschalom and D. P. Di Vincenzo, Phys. Today **48** (4), 43 (1995).

[4] D. L. Leslie-Pelecky and R. D. Rieke, Chem. Mater. **8**, 1770 (1996).

[5] A. D. Kent, S. von Molnar, S. Gider, and D. D. Awschalom, J. Appl. Phys. **76**, 6656 (1994).

[6] D. Gatteschi, A. Caneschi, L. Pardi, and R. Sessoli, Science **265**, 1054 (1994).

[7] A. L. Barra, P. Debrunner, D. Gatteschi, C. E. Schulz, and R. Sessoli, Europhys. Lett. **35**, 133 (1996); C. Sangregorio, D. Gatteschi, R. Sessoli, T. Ohm, and P. Paulsen, Phys. Rev. Lett. **78**, 4645 (1997).

[8] R. Sessoli, Mol. Cryst. Liq. Cryst. Sci. Technol., Sect. A **274**, 145 (1995).

[9] H. J. Eppley, H.-L. Tsai, N. de Vries, K. Folting, G. Christou, and D. N. Hendrickson, J. Am. Chem. Soc. **117**, 301 (1995).

[10] T. Lis, Acta Crystallogr. Sect. B **36**, 2042 (1980).

[11] A. Caneschi, D. Gatteschi, R. Sessoli, A. L. Barra, L. C. Brunel, and M. Guillot, J. Am. Chem. Soc. **113**, 5873 (1991).

[12] R. Sessoli, D. Gatteschi, A. Caneschi, and M. A. Novak, Nature (London) **365**, 141 (1993).

[13] C. Paulsen, J.-G. Park, B. Barbara, R. Sessoli, and A. Caneschi, J. Magn. Magn. Mater. **140**, 1891 (1995); C. Paulsen and J.-G. Park, in *Quantum Tunneling of the Magnetization* (Ref. 2), p. 189.

[14] M. A. Novak and R. Sessoli, in *Quantum Tunneling of the Magnetization* (Ref. 2), p. 171.

[15] J. R. Friedmann, M. P. Sarachik, J. Tejada, and R. Ziolo, Phys. Rev. Lett. **76**, 3830 (1996).

[16] L. Thomas, F. Lionti, R. Ballou, D. Gatteschi, R. Sessoli, and B. Barbara, Nature (London) **383**, 145 (1996).

[17] P. Politi, A. Rettori, F. Hartmann-Boutron, and J. Villian, Phys. Rev. Lett. **75**, 537 (1995).

[18] J. Villain, F. Hartmann-Boutron, R. Sessoli, and A. Rettori, Europhys. Lett. **27**, 159 (1994).

[19] A. L. Burin, N. V. Prokof'ev, and P. C. E. Stamp, Phys. Rev. Lett. **76**, 3040 (1996); P. Politi, A. Rettori, F. Hartmann-Boutron, and J. Villain, *ibid.* **76**, 3041 (1996); P. C. E. Stamp, Nature (London) **383**, 125 (1996); E. M. Chudnovsky, Science **274**, 938 (1996); F. Hartmann-Boutron, J. Phys. IV **6**, 137 (1996).

[20] R. Sessoli, H. L. Tsai, A. R. Shake, S. Wang, J. B. Vincent, K. Folting, D. Gatteschi, G. Christou, and D. N. Hendrickson, J. Am. Chem. Soc. **115**, 1804 (1993).

[21] F. Muller, M. A. Hopkins, N. Coron, M. Grynberg, J. C. Brunel, and G. Martinez, Rev. Sci. Instrum. **60**, 3681 (1989); A. L. Barra, L. C. Brunel, and J. B. Robert, Chem. Phys. Lett. **165**, 107 (1990).

[22] C. J. H. Jacobsen, E. Pedersen, J. Villadsen, and H. Weihe, Inorg. Chem. **32**, 1216 (1993).

[23] A. Abragam and B. Bleaney, *Electron Paramagnetic Resonance of Transition Ions* (Dover, New York, 1986).

[24] A. Bencini and D. Gatteschi, *EPR of Exchange Coupled Systems* (Springer-Verlag, Berlin, 1990).

[25] B. McGarvey, in *Transition Metal Chemistry*, edited by R. L.

Carlin (Marcel Dekker, New York, 1966), Vol. 3.
[26] H. J. Gerritsen and E. S. Sabisky, Phys. Rev. **132**, 1507 (1963).
[27] dbm = 1,3-diphenyl-1,3-propanedionate. A. L. Barra *et al.*, Angew. Chem. Int. Ed. Engl. (to be published).
[28] F. Hartmann-Boutron, P. Politi, and J. Villain, Int. J. Mod. Phys. B **10**, 2577 (1996).
[29] J. M. Hernandez, X. X. Zhang, F. Luis, J. Bartolomé, J. Tejada, R. Ziolo, Europhys. Lett. **35**, 301 (1996); F. Luis, J. Bartolomé, J. F. Fernàndez, J. Tejada, J. M. Hernàndez, X. X. Zhang, and R. Ziolo, Phys. Rev. B **55**, 11 448 (1997).
[30] A. Fort, A. Rettori, J. Villain, D. Gatteschi, and R. Sessoli (unpublished).